Simulating Urban Growth and Land Degradation in Bosso, Nigeria: A CA-Markov Framework for Localized Climate-Resilient Planning

Ekundayo Abayomi ADESINA, Nigeria; Oluibukun Gbenga AJAYI, Joseph Olayemi ODUMOSU, Namibia; Joshua EZEANYA, Nigeria

Correspondence Address: adesinageoworldsolutions@gmail.com

Keywords: Cellular Automata, Geospatial Analysis, Land Use Land Cover Change, Markov-CA Model, Remote Sensing, Urban Expansion.

SUMMARY

Rapid urbanisation in sub-Saharan Africa poses pressing sustainability challenges, yet district-level predictive modelling, essential for local climate adaptation planning, remains limited. This study addresses this gap by applying a high-accuracy Cellular Automata-Markov (CA-Markov) model to simulate past and future land use/land cover (LULC) changes in Bosso Local Government Area, Niger State, Nigeria (2000-2030). Using Landsat imagery, we classified five LULC classes and achieved robust validation (kappa = 0.973, overall accuracy = 95.37%). Results show a striking expansion of bare surface, projected to reach 88.91% by 2030, and a sharp decline in agricultural land to 1.08%. The primary contribution of this study is a methodological innovation: a replicable, high-accuracy, and policy-integrated CA-Markov framework that advances the technique from predictive modelling to a scalable decision-support tool for climate-resilient planning in data-scarce regions. Unlike typical applications that end with prediction, our framework provides a validated protocol for embedding geospatial projections directly into statutory planning, offering a transferable template for sustainable urban governance across sub-Saharan Africa's dryland cities. Unlike typical applications that end with prediction, our framework provides a validated protocol for embedding projections directly into statutory planning. It provides a transferable template for embedding geospatial projections into sustainable urban planning in data-scarce regions. The findings highlight the urgent need for green infrastructure, soil conservation, and targeted land-use zoning. These evidence-based insights directly support Sustainable Development Goals 11, 13, and 15 and offer a locally adaptable model for other rapidly urbanising dryland regions in sub-Saharan Africa.

Simulating Urban Growth and Land Degradation in Bosso, Nigeria: A CA-Markov Framework for Localized Climate-Resilient Planning

Ekundayo Abayomi ADESINA, Nigeria; Oluibukun Gbenga AJAYI, Joseph Olayemi ODUMOSU, Namibia; Joshua EZEANYA, Nigeria

1. INTRODUCTION

Rapid urban growth has become a crucial driver of climate change impacts, particularly in Africa, where urbanization rates outpace infrastructural and environmental planning capacities (Cobbinah and Finn, 2023; Ayeni *et al.,* 2025). Cities in sub-Saharan Africa, including Nigeria, face compounding pressures from population influxes, informal settlements, and land-use changes, which exacerbate vulnerabilities to extreme climate events such as flooding, heatwaves, and prolonged droughts (Andreasen *et al.,* 2023; Cinderby *et al.,* 2024; Adesina *et al.,* 2025). These dynamics disrupt ecosystems, intensify urban heat islands, and strain water resources, disproportionately affecting low-income communities (Idowu and Olalekan, 2025; Mutale & Ajayi, 2026). Such trends highlight the urgent need to integrate climate resilience into urban development frameworks (Rezvani *et al.,* 2023; Benade *et al.*, 2026).

Given the numerous factors influencing sustainable development, policy formulators and decision-makers require precise information on the present and future status (Jimenez-Espada *et al.,* 2023; Karimi *et al.,* 2025). Therefore, changes in Land Use and Land Cover (LULC) and future LULC modelling have gained traction in recent years. As evidenced by the studies of Aburas et al. (2021), Azabdaftari and Sunar (2024)**,** and Sumari *et al.* (2025), numerous researchers have focused on examining urban expansion using various methodologies.

Remote sensing methods are now quite successful in identifying changes brought on by urban growth. This approach has been widely used in urban expansion studies over the past few decades in conjunction with Geographic Information Systems (GIS) (Du *et al.,* 2014; Singh *et al.,* 2022). Given the substantial impacts of LULC change and urban growth, it is imperative to comprehend, predict, and project land dynamics at regional and global levels (AbdelRahman, 2023). Researchers have recently examined potential LULC changes using several models, thereby offering policymakers and urban planners' information to promote sustainable urban growth (Masoudi *et al.,* 2021). Markov Chain (MC) and Cellular Automata (CA) are two of these modelling approaches that have grown in popularity (Jimenez-Lopez, 2022; Adesina *et al.*, 2026). While MC models examine the probability of changes in land cover, CA models are chosen for their capacity to combine temporal and geographical features of processes (Wellmann *et al.,* 2020; Blanco *et al.,* 2024).

While CA-Markov models are widely applied globally, their transformation into actionable, district-level planning tools in West Africa remains limited. This study bridges this gap by introducing a calibrated, high-resolution modelling framework designed explicitly for transferability to secondary cities in data-scarce dryland regions. Our approach moves beyond mere prediction to deliver a policy-integrated workflow that aligns with local resilience frameworks, thereby addressing a critical gap in climate adaptation planning. Most existing studies focus on metropolitan or regional scales, often overlooking local socio-ecological specificities critical for policy implementation.

This study bridges this gap by developing and validating a high-resolution, localized CA-Markov model for Bosso LGA that not only predicts LULC changes with exceptional accuracy but also translates projections into concrete, context-specific interventions aligned with Niger State's urban resilience frameworks. More broadly, it presents a methodological innovation: a calibrated and validated modelling template designed explicitly for transferability to similar secondary cities across West Africa's drylands, where data scarcity and planning capacity are shared constraints.

Specifically, we aim to: (1) analyze the spatiotemporal dynamics of LULC in Bosso LGA from 2000 to 2020; (2) develop and validate a high-accuracy CA-Markov model for the region; (3) project LULC for 2030; and (4) derive evidence-based, localized recommendations for sustainable urban planning and climate resilience.

2. STUDY AREA

Bosso Local Government Area, established in 1991, is situated at latitude 9°14'00" N and longitude 6°28'20"E, with a population of 147,359 (NPC, 2006). Primarily inhabited by the Gwari people, along with other ethnic groups like the Nupe, Hausa, Koro, Kadara, and Yoruba, the area experiences a typical Niger State climate characterized by a yearly mean temperature ranging from 21.11°C to 37.78°C and an annual rainfall of approximately 680 millimetres. The rainy season, extending from March to November, supports rain-fed agriculture, the primary occupation for both men and women. Figure 1 provides a visual representation of the study area.

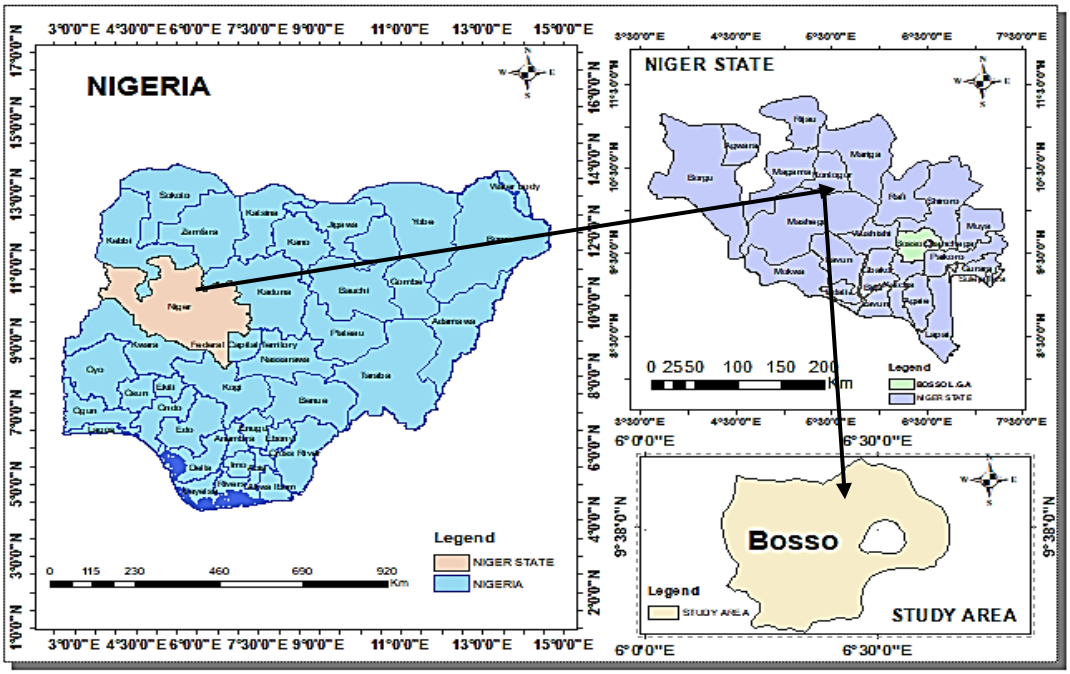

Figure 1**:** Study Area Map (Bosso Local Government Area, Niger State, Nigeria)

3. METHODOLOGY

3.1 Data Collection and Pre-Processing

This study evaluated the dynamic changes in land use and land cover resulting from population growth between 2000 and 2020. Multi-temporal Landsat satellite images (Landsat 7 ETM+ for 2000 and 2010, and Landsat 8 OLI/TRS for 2020) were acquired from the USGS Earth Explorer portal (path 190, row 54). All images were from the dry season (November-February) to minimize seasonal vegetation variation. Geometric and atmospheric corrections were performed using the Semi-Automatic Classification Plugin (SCP) in QGIS 3.28. The Dark Object Subtraction (DOS) method was applied for atmospheric correction (Frazier and Hemingway, 2021). Image enhancement was conducted by creating false-colour composites (bands 5, 4, 3 for Landsat 7 and bands 6, 5, 4 for Landsat 8) to improve visual interpretability for training site selection.

3.2 Image Classification and Accuracy Assessment

Image classification aimed to automatically categorize each pixel into specific land cover classes (Li *et al.,* 2021; Yasrebi *et al.,* 2025). A supervised classification approach utilizing the Maximum Likelihood Classifier (MLC) in ArcGIS 10.8 was employed. Five LULC classes were defined based on visual and digital interpretation: Vegetation, Built-up Area, Bare Soil, Agricultural Land, and Water Bodies. The description of these classes is provided in Table 1. Training samples (minimum of 50 polygons per class) were collected based on visual interpretation and local knowledge. The classified images for 2000, 2010, and 2020 were generated.

Table 1: Various land use types in the study area (adapted from Lillesand *et al.,* 2015)

Land use types	Descriptions
Built up area	These include residential, commercial and service, transportation, communication and utilities, and industrial and commercial complexes.
Bare surface	These also include dry salt flats, beaches, sandy areas other than beaches, bare exposed rocks, strip mines, queries, and gravel pits.
Agricultural land	These are cropland, pasture, orchard, nurseries, and ornamental agricultural areas.
Vegetation	This includes areas of the natural vegetation of any plant species, trees, and deciduous and ever-greened forest lands.
Water bodies	These involve areas persistently lodged with waters such as streams, canals, lakes, reservoirs, bays, and estuaries.

Accuracy assessment was performed using a stratified random sampling technique, selecting 200 reference points per epoch. These points were compared against high-resolution Google Earth imagery and field knowledge. A confusion matrix was generated to compute Overall Accuracy, Producer's Accuracy, User's Accuracy, and the Kappa Coefficient (K). The Kappa coefficient was calculated in Equation (1):

$$K = \frac{N\sum_{i=1}^{r} x_{ii} - \sum_{i=1}^{r}(x_{i+} * x_{+i})}{N^2 - \sum_{i=1}^{r}(x_{i+} * x_{+i})} \quad (1)$$

Where:
N is the total number of observations,
r is the number of rows in the matrix,
x_{ii} is the number of observations in row i and column i,
x_i is the marginal total of row i,
x_{+i} is the marginal total of column i,

The interpretation of the Kappa coefficient is presented in Table 2.

Table 2: Kappa coefficient statistics interpretation (Zhang *et al.,* 2023)

S/N	Kappa value	Interpretation
1	<0.00	No agreement
2	0.0-0.20	Slight agreement
3	0.21-0.40	Fair agreement
4	0.41-0.60	Moderate agreement
5	0.61-0.80	Substantial agreement
6	0.81-1.00	Almost perfect agreement

3.3 Change Detection and Trend Analysis

To quantify the rate and trend of LULC change, an area-based change analysis was conducted. The area (in km²) and percentage of each class for 2000, 2010, and 2020 were computed. The annual rate of change for a class was calculated in Equation (2):

$$\text{Annual Rate of Change (\%)} = \left(\frac{A_t - A_{t0}}{A_{t0}}\right) * \frac{1}{T} * 100\% \qquad (2)$$

where A_t and A_{t0} are the areas at the initial and final times, and T is the time interval in years. A transition matrix was also generated for the period 2000-2020 to show the proportion of each class that changed to another class.

3.4 CA-Markov Model Implementation and Projection

The CA-Markov model, implemented using the CA-Markov module in IDRISI TerrSet 18.31, was used to project LULC for 2030. The process involved two main steps:

(i) Markov Chain Analysis: A transition probability matrix P and a transition areas matrix were generated from the 2000 and 2010 LULC maps. The probability P_{ij} of a pixel transitioning from state i to state j over the 10-year interval is given in Equation (3):

$$P_{ij} = \frac{n_{ij}}{N_i} \qquad (3)$$

where n_{ij} is the number of pixels that transitioned from class i to class j, and N_i is the total number of pixels originally in class i.

(ii) Cellular Automata Simulation: The spatial contiguity of changes was modelled using a Cellular Automata filter. A 5×5 contiguity filter was selected to define the cellular neighborhood, a common choice in CA-Markov applications that balances spatial contextual information with computational efficiency (Wellmann *et al.,* 2020). This filter size adequately captures local land-use transitions influenced by adjacent cells, which is crucial for simulating urban expansion patterns in a peri-urban setting like Bosso LGA.

The CA model allocates future changes based on the suitability of locations, which is influenced by the Markovian transition probabilities and the state of neighbouring cells. The model was validated by running it from 2000 to predict the 2020 LULC, and comparing the simulation to the actual 2020 classification. The validated model, with a Kappa index of agreement of 0.973, was then used to project LULC for 2030 by running it for a single 10-year iteration (2020-2030). While the CA-Markov model operates on spatially explicit transition rules, this study focuses on validating the modelling framework, presenting authoritative quantitative trends, and translating results into evidence-based policy insights. Therefore, the comprehensive quantitative projections are presented in Table 6, and a detailed narrative description of the dominant spatial patterns, logically inferred from the model's calibrated transition rules and the historical spatial trajectories shown in Figure 3, is provided in Section 4.5.

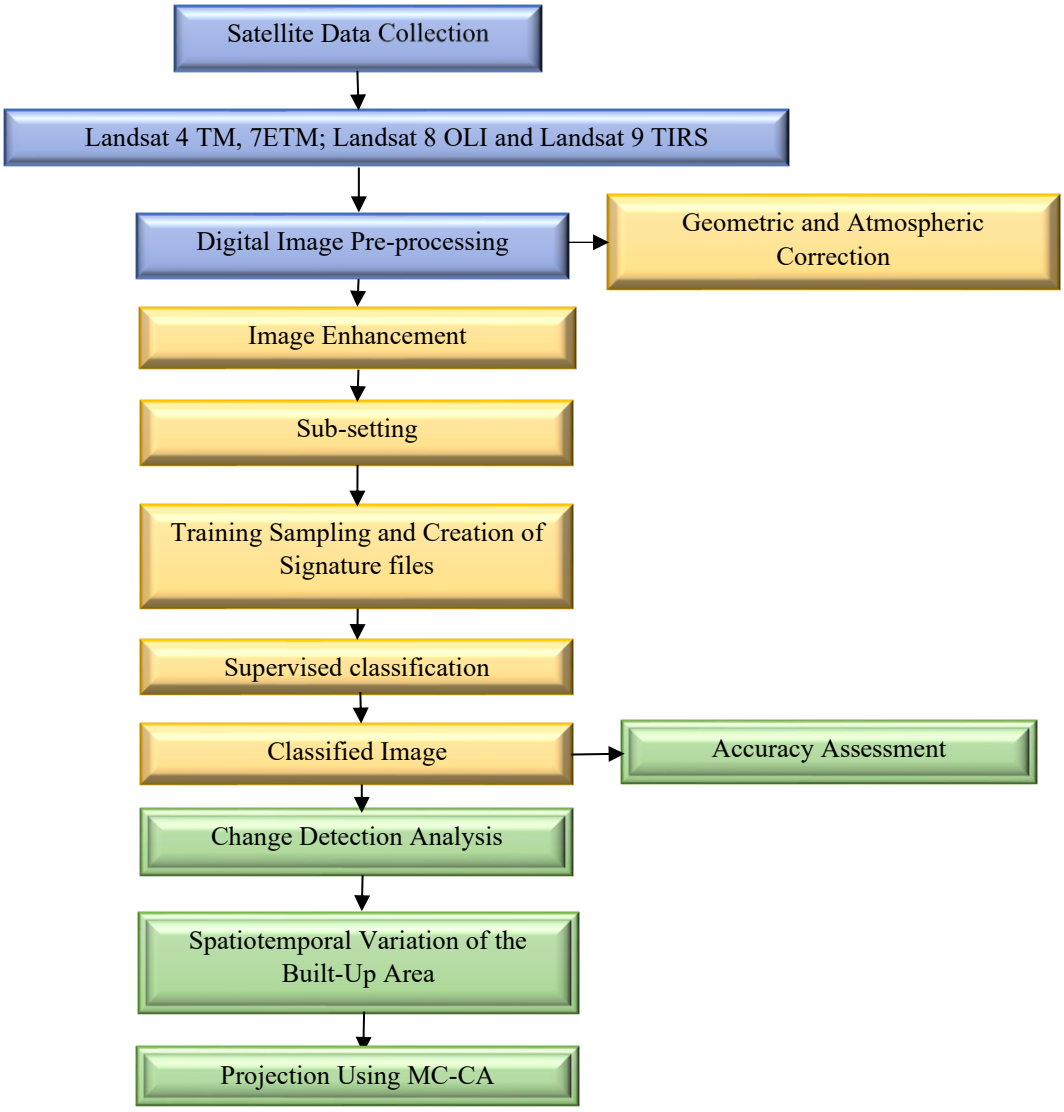

Figure 2: Methodology flow diagram process for the study

3.5 Innovative Aspects of the Applied CA-Markov Framework

This study advances CA-Markov modelling through three core methodological innovations designed for scalability and policy relevance: (1) achieving exceptional predictive accuracy (Kappa > 0.97) using widely accessible Landsat data; (2) embedding model outputs directly into existing local planning instruments; and (3) providing a transferable calibration template adaptable by municipalities across West Africa. This framework shifts the application from academic simulation to actionable urban governance.

4. RESULTS

4.1 Land Use Land Cover Change Dynamics (2000-2020)

Land use/land cover maps for the years 2000, 2010, and 2020 were generated (Figure 3), illustrating the temporal changes. A detailed analysis of the area changes is presented in Table 3.

Table 3: Land use land cover change dynamics of the study area (2000-2020)

Classes	2000 Area (km²)	2000 %	2010 Area (km²)	2010 %	2020 Area (km²)	2020 %
Agricultural land	974.759	58.54	886.818	53.26	633.758	38.06
Bare surface	591.262	35.51	672.180	40.37	924.108	55.50
Built-up area	41.414	2.49	59.395	3.57	69.900	4.20
Natural vegetation	51.238	3.08	42.760	2.57	33.715	2.02
Water bodies	6.524	0.39	4.032	0.24	3.726	0.22

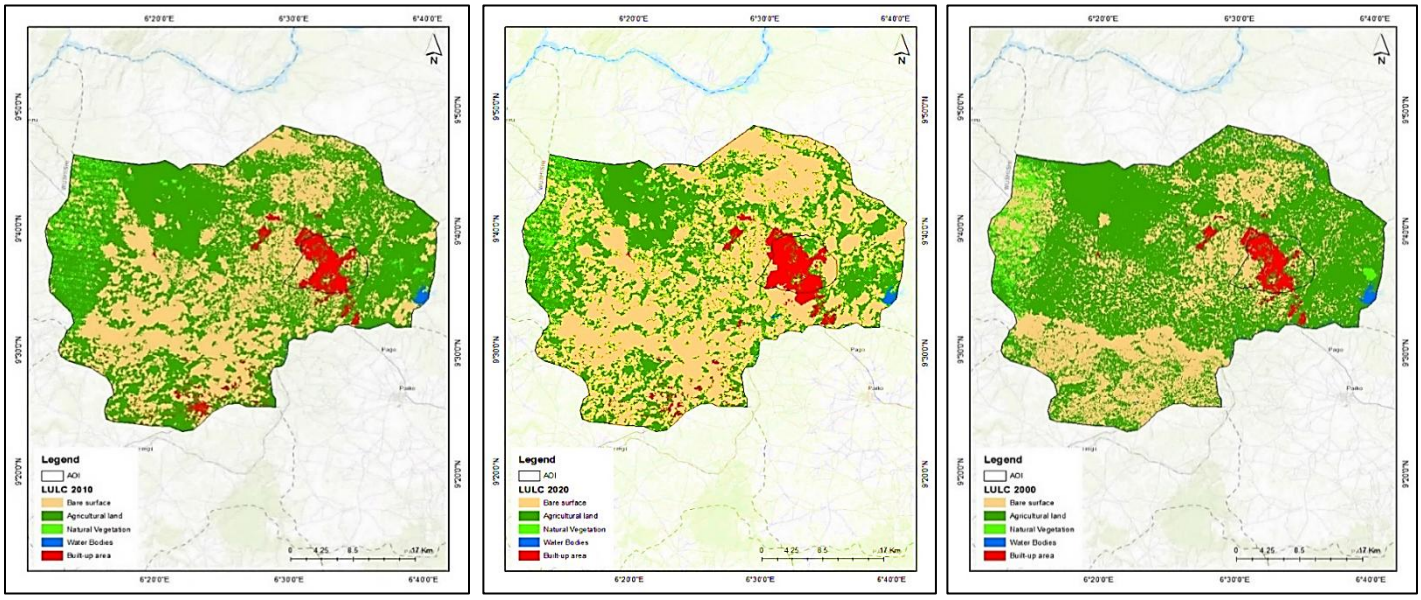

(a) LULC map for 2000 (b) LULC map for 2010 (c) LULC map for 2020

Figure 3: Historical LULC Maps for Bosso LGA (2000, 2010, 2020) and Basis for 2030 Spatial Projection

The spatial patterns of change from (a) 2000 to (c) 2020, particularly the conversion of Agricultural Land (green) to Bare Surface (beige) and the expansion of Built-up Areas (red), provide the spatial basis for the 2030 projections summarized in Table 6 and described spatially in Section 4.5. The 2030 projection indicates an intensification of these patterns, with Bare Surface becoming dominant across central and eastern zones.

4.2 Change Detection and Transition Analysis

The transition probability matrix, showing gains and losses between 2000-2010 and 2010-2020, is presented in Table 4. The most significant change was the conversion of Agricultural Land to Bare Surface. Figure 4 presents the gains and losses between 2000 and 2010, and 2010 and 2020 obtained from the study.

Table 4: Transition matrix showing area changes (km²) between 2000-2010 and 2010-2020

Period	Class	Area Change (km²)	% Change	Annual Rate (%)
2000-2010	Agricultural Land	-87.941	-5.28	-0.528
	Bare Surface	+80.918	+4.86	+0.486
	Built-up Area	+17.981	+1.08	+0.108
	Natural Vegetation	-8.478	-0.51	-0.051
	Water Bodies	-2.492	-0.15	-0.015
2010-2020	Agricultural Land	-253.060	-15.20	-1.520
	Bare Surface	+251.928	+15.13	+1.513
	Built-up Area	+10.505	+0.63	+0.063
	Natural Vegetation	-9.045	-0.55	-0.055
	Water Bodies	-0.306	-0.02	-0.002

Figure 4: Gains and losses between 2000 and 2010, and 2010 and 2020

4.3 Transition Statistics for Each Land Use Class (2000-2020)

Analysis of the full transition matrix for 2000-2020 revealed the dominant land conversion pathway. The key finding was that 435.57 km² of agricultural land transitioned to bare surface, representing the largest single land conversion during the study period.

Table 5: Projected distribution of LULC for 2030 compared to historical data

Classes	2000 Area (km²)	2000 %	2010 Area (km²)	2010 %	2020 Area (km²)	2020 %	2030 Area (km²)	2030 %
Agricultural land	974.759	58.54	886.818	53.26	633.758	38.06	17.988	1.08
Bare surface	591.262	35.51	672.180	40.37	924.108	55.50	1480.570	88.91
Built-up area	41.414	2.49	59.395	3.57	69.900	4.20	102.639	6.16
Natural vegetation	51.238	3.08	42.760	2.57	33.715	2.02	59.398	3.57
Water bodies	6.524	0.39	4.032	0.24	3.726	0.22	4.694	0.28

4.4 Model Validation and 2030 Projection

The projected LULC distribution for 2030 is presented in Table 6.

Table 6: Projected distribution of LULC for 2030 compared to historical data

Year	2000	2010	2020	2030 (Projected)				
Classes	**Area (km²)**	**%**	**Area (km²)**	**%**	**Area (km²)**	**%**	**Area (km²)**	**%**
Agricultural land	974.759	58.54	886.818	53.26	633.758	38.06	17.988	1.08
Bare surface	591.262	35.51	672.180	40.37	924.108	55.50	1480.570	88.91
Built-up area	41.414	2.49	59.395	3.57	69.900	4.20	102.639	6.16
Natural vegetation	51.238	3.08	42.760	2.57	33.715	2.02	59.398	3.57
Water bodies	6.524	0.39	4.032	0.24	3.726	0.22	4.694	0.28
Total	**1665.206**	**100**	**1665.206**	**100**	**1665.206**	**100**	**1665.206**	**100**

4.5 Spatial Patterns of Projected LULC Change (2030)

The projected LULC distribution for 2030 (Table 6) reveals not only quantitative shifts but also distinct spatial patterns, which can be inferred from the historical trajectory visualized in Figure 3. The model projects that the striking expansion of Bare Surface (to 88.91%) will be most pronounced in the central and eastern zones of Bosso LGA, areas visible in Figure 3c (2020) as currently transitioning from agricultural land (green) to bare soil (beige). Built-up area growth (projected to reach 6.16%) is expected to cluster as a contiguous expansion around existing urban cores in the west (visible as red patches in Figure 3c) and extend linearly along major transportation corridors (e.g., the Minna-Bida Road). The minimal remaining Agricultural Land (1.08%) is projected to persist as fragmented patches in the northern sector, while the slight recovery of

Natural Vegetation is likely in scattered, abandoned plots in the southeastern zone. These projected spatial trends, extrapolated from the validated 2000-2020 model, underscore the critical need for targeted, location-specific interventions in land-use zoning and climate adaptation planning.

5. DISCUSSION

5.1 Interpretation of Observed LULC Changes (2000-2020)

The observed LULC changes in Bosso from 2000 to 2020 (Table 3, Figure 3) align with broader urbanization trends in sub-Saharan Africa but exhibit critical local specificities. The marked decline in Agricultural Land (from 58.54% to 38.06%) and Natural Vegetation (from 3.08% to 2.02%), coupled with the rise in Built-up Area (from 2.49% to 4.20%) and especially Bare Surface (from 35.51% to 55.50%), points to a complex impact of the drivers (Kogan, 2023).

The expansion of built-up areas is attributable to Bosso's role as an administrative and commercial hub within Niger State, which accelerates migration and infrastructure development (Abubakar *et al.,* 2025). However, the most striking transformation is the massive conversion of Agricultural Land to Bare Surface, as quantified by the conversion of 435.57 km² of agricultural land to bare surface. Between 2000 and 2020, 435.57 km² of agricultural land became bare surface, the largest single transition recorded. This trend is further illustrated in the change-detection bar chart (Figure 4), which shows consistent gains in bare surface at the direct expense of agricultural land in both periods (2000-2010 and 2010-2020).

This expansion of Bare Surface suggests severe land degradation, likely driven by unsustainable farming practices, soil erosion, land abandonment, and climate variability with reduced rainfall (IPCC, 2023; Tefera *et al.,* 2024). Analysis of the transition matrix (Table 4) reveals that while some bare surface did revert to agriculture (91.76 km²) or become built-up (19.24 km²), the net change remained overwhelmingly toward bare land.

Compared to similar studies, the rate of urban expansion in Bosso (a 1.71-percentage-point increase in built-up area over 20 years) is less dramatic than in some Asian megacities (e.g., Yang *et al.,* 2025 reported 69.6% growth in Xi'an) but is consistent with patterns in other African secondary cities such as Dodoma, Tanzania (Sumari, 2025). However, the extreme conversion to Bare Surface is a distinctive and concerning finding that sets Bosso apart and warrants urgent policy attention (Ben-Enukora and Ejem, 2024).

5.2 Model Performance and Projection Reliability

The high validation accuracy (K= 0.973, overall accuracy = 95.37%) of the CA-Markov model confirms its robustness for simulating LULC change in Bosso. This performance is comparable to or exceeds the accuracy reported in similar studies (e.g., Aburas *et al.,* 2021; Hossain *et al.* (2020) reported an overall accuracy of 83%). The model's strength lies in its integration of temporal transition probabilities (the Markov chain) with spatial neighborhood rules (the cellular automaton), making it particularly suitable for capturing the spatial complexity of urban growth in a data-scarce context (Ilori *et al.* (2019). The validation was performed by simulating the 2020 map from 2000 data and comparing it with the actual classified 2020 map (Figure 3c). The close

agreement demonstrates that the model can reliably replicate past transitions, thereby lending credibility to the 2030 projection (Pang *et al.,* 2022).

5.3 Implications of the 2030 Projection and Evidence-Based Recommendations

While focused on Bosso LGA, the trends and methodology have significant regional implications. The observed rapid conversion of agricultural land to bare surface mirrors patterns observed in dryland regions across Mali and Burkina Faso, suggesting a broader West African syndrome of peri-urban land degradation. The developed modelling framework is deliberately designed for adaptation to similar contexts where moderate-resolution Landsat data is the primary source. The 2030 projection (Table 6) presents a critical scenario for urban and environmental planners. The continued expansion of Built-up Area to 6.16% (102.64 km²) underlines persistent urbanization pressure (Kemajou *et al.,* 2021).

However, the most alarming projection is the dominance of Bare Surface, predicted to cover 88.91% (1,480.57 km²) of the LGA. It is important to frame this extreme projection as a rigorous "business-as-usual" scenario derived from the powerful, recent historical trend (2000-2020). Its primary value lies not as an inevitability, but as a stark, evidence-based warning signal that demands immediate policy intervention to alter the current trajectory of land degradation. Agricultural land is projected to plummet to only 1.08% (17.99 km²), a near-complete collapse of this land-use class (Nnanguma, 2025).

While this extreme projection is influenced by the strong historical trend of agricultural land degradation seen in Tables 3 and 5, it signals potential large-scale land degradation and its cascading consequences, such as increased surface runoff and flood risk, intensified urban heat island effect, loss of soil fertility, and reduced carbon sequestration (Nunes *et al.,* 2022; Ajayi *et al.*, 2023). The projected dominance of bare surface (88.91% by 2030) and near-total loss of agricultural land are alarming indicators of unsustainable land management. These trends are not merely statistical outcomes but reflect deeper systemic issues, unsustainable farming, soil erosion, land abandonment, and inadequate land-use zoning. To counteract these trajectories, we propose the following evidence-based interventions, directly derived from our model outputs:

1. **Priority Restoration Zones:** Target the 435.57 km² of former agricultural land now classified as bare surface (Table 5) for large-scale afforestation and soil-conservation projects.
2. **Green Infrastructure Integration:** Mandate green corridors, parks, and permeable surfaces within new developments (projected built-up expansion in Table 6) to mitigate urban heat and runoff. The model's spatial output (described in Section 3.4) identifies western and corridor-adjacent zones as hotspots for green-space integration.
3. **Agricultural Land Protection:** Implement strict zoning laws to protect the remaining stable agricultural patches, informed by transition probabilities in Table 4.
4. **Climate-Resilient Planning:** Integrate the 2030 LULC map into Bosso's urban master plan, ensuring new infrastructure is sited to minimize environmental impact and designed for flood resilience, given the increased runoff expected from expanded bare surfaces.

5. **Policy Integration and Monitoring:** Integrate the 2030 LULC projections into Niger State's Urban Development Master Plan and the State Climate Action Policy. Establish a participatory monitoring framework involving local communities, planners, and environmental agencies to track land degradation and green infrastructure outcomes.

5.4 Broader Implications and Transferability of the Framework

The modelling framework presented is intentionally designed for adaptation to analogous dryland urban contexts, where moderate-resolution Landsat data is often the only viable source. This study presents a transferable blueprint for integrating predictive geospatial modelling into climate adaptation and land-use planning processes across sub-Saharan Africa by providing a stepwise, transparent methodology validated with high accuracy. The framework's integration with local policy (Section 3.5) is a crucial component of this transferability, ensuring the scientific output is primed for governance applications.

5.5 Study Limitations and Future Research Directions

Limitations include: (1) moderate-resolution Landsat imagery may not capture small-scale features; (2) the model does not explicitly incorporate socio-economic drivers; (3) projections would benefit from participatory ground-truthing. Future research should integrate higher-resolution satellite data (e.g., Sentinel-2) to capture small-scale urban features and incorporate socio-economic drivers such as population density, land value, and policy scenarios into the CA-Markov framework. Participatory ground-truthing and community engagement in model calibration would further enhance the relevance and accuracy of projections for local planning.

6. CONCLUSION AND RECOMMENDATIONS

This study demonstrates that a high-accuracy CA-Markov model, when calibrated for local contexts and integrated into policy frameworks, serves as a transformative decision-support tool for sustainable urban governance. The validated framework provides a replicable template for other sub-Saharan African cities, enabling proactive, evidence-based land-use management that balances urban growth with climate resilience and environmental sustainability. The validation performance ($K = 0.973$) confirms its reliability for simulating LULC dynamics in rapidly urbanizing districts like Bosso LGA, Nigeria. The primary innovation lies in its dual function: as a high-fidelity simulation tool for a specific locality, and as a replicable, policy-integrated framework for regional application. The projections reveal unsustainable trajectories that demand integrated policy responses. The methodology provides a scalable and transferable template for other sub-Saharan African cities, enabling proactive, evidence-based land-use management that balances growth with sustainability and resilience.

REFERENCES

AbdelRahman, M. A. (2023). An overview of land degradation, desertification and sustainable land management using GIS and remote sensing applications. *Rendiconti Lincei. Scienze Fisiche e Naturali*, *34*(3), 767-808.

Abubakar, I. R., Onyebueke, V. U., Lawanson, T., Barau, A. S., & Bununu, Y. A. (2025). Urban planning strategies for addressing climate change in Lagos megacity, Nigeria. *Land Use Policy*, *153*, 107524.

Aburas, M. M., Ho, Y. M., Pradhan, B., Salleh, A. H., & Alazaiza, M. Y. (2021). Spatio-temporal simulation of future urban growth trends using an integrated CA-Markov model. *Arabian Journal of Geosciences*, *14*(2), 131.

Adesina, E. A., Ajayi, O. G., Odumosu, J. O., & Taiwo, E. O. (2026). Dynamic suitability-weighted CA-Markov model for projecting urban growth and thermal impacts: a case study of Abuja. *Nova Geodesia*, 6(1), 475. https://doi.org/10.55779/ng61475

Adesina, E. A., Odumosu, J. O., Ajayi, O. G., Musa, A., Onuigbo, I. C., & Adesiji, A. R. (2025). Evaluating the impact of the Spatial resolution of digital elevation models on flood modelling. *Water Resources Management*, 1-32. https://doi.org/10.1007/s11269-025-04206-6

Ajayi, O. G., Kolade, T. S., Baba, M. (2023). Mapping and assessing the seasonal dynamics of surface urban heat intensity using LandSAT-8 OLI/TIRS images. In J. C. Egbueri et al. (eds.), Climate Change Impacts on Nigeria, Springer Climate, 261-278. https://doi.org/10.1007/978-3-031-21007-5_14

Andreasen, M. H., Agergaard, J., Allotey, A. N., Møller-Jensen, L., & Oteng-Ababio, M. (2023). Built-in flood risk: The intertwinement of flood risk and unregulated urban expansion in African cities. *Urban Forum*, *34*(3), 385-411.

Ayeni, A. O., Aborisade, A. G., Aiyegbajeje, F. O., & Soneye, A. S. O. (2025). The dynamics of peri-urban expansion in sub-Saharan Africa: Implications for sustainable development in Nigeria and Ghana. *Discover Sustainability*, *6*(1), 290.

Azabdaftari, A., & Sunar, F. (2024). Predicting urban tomorrow: CA-Markov modelling and district evolution. *Earth Science Informatics*, *17*(4), 3215–3232.

Benade, R., Ajayi, O., & Makando, I. (2026). Climate induced land degradation in Namibia: Towards resilient and equitable land governance. *African Journal on Land Policy and Geospatial Sciences*, 9(3), 494–523. https://revues.imist.ma/index.php/AJLP-GS/article/view/63234

Ben-Enukora, C. A., & Ejem, A. A. (2024, April). *Environmental responsiveness towards desertification and land degradation: A review of literature on restoration strategies in dryland communities in Africa*. Paper presented at the 2024 International Conference on Science, Engineering and Business for Driving Sustainable Development Goals (SEB4SDG).

Budnukaeku, A. C., & Emmanuel, O. S. (2024). Historical Analysis of Climate Variability and Agricultural Production in Nigeria (1931-2020). *Journal of World Economy*, *3*(3), 1-14.

Cinderby, S., Haq, G., Opiyo, R., Muhoza, C., Ngabirano, A., Wasike, Y., & Cambridge, H. (2024). Inclusive climate resilient transport challenges in Africa. *Cities*, *146*, 104740.

Cobbinah, P. B., & Finn, B. M. (2023). Planning and climate change in African cities: Informal urbanization and 'Just' Urban transformations. *Journal of Planning Literature*, *38*(3), 361-379.

Du, P., Liu, P., Xia, J., Feng, L., Liu, S., Tan, K., & Cheng, L. (2014). Remote sensing image interpretation for urban environment analysis: Methods, system and examples. *Remote Sensing*, *6*(10), 9458-9474.

Frazier, A. E., & Hemingway, B. L. (2021). A technical review of planet smallsat data: Practical considerations for processing and using planetscope imagery. *Remote Sensing*, *13*(19), 3930.

Hossain, A., Krupnik, T. J., Timsina, J., Mahboob, M. G., Chaki, A. K., Farooq, M., & Hasanuzzaman, M. (2020). Agricultural land degradation: Processes and problems undermining future food security. In *Environment, climate, plant and vegetation growth* (pp. 17-61). Springer International Publishing.

Idowu, O. O., & Olalekan, O. (2025). Influence of Land Use Land Cover Change on Urban Heat Island Intensity in Ikeja Local Government Area, Lagos State. *FUOYE Planning Journal*, *3*(1).

Ilori, C. O., Pahlevan, N., & Knudby, A. (2019). Analyzing performances of different atmospheric correction techniques for Landsat 8: Application for coastal remote sensing. *Remote Sensing*, *11*(4), 469.

Lee, H., Calvin, K., Dasgupta, D., Krinner, G., Mukherji, A., Thorne, P., & Park, Y. (2023). *IPCC, 2023: Climate change 2023: Synthesis report, summary for policymakers*. IPCC.

Jiménez-Espada, M., Martínez García, F. M., & González-Escobar, R. (2023). Sustainability indicators and GIS as land-use planning instrument tools for urban model assessment. *ISPRS International Journal of Geo Information*, *12*(2), 42.

Jiménez-López, E. (2022, June). *Inverse filter in the growth of urban sprawl with cellular automata model*. Paper presented at the Second International Conference on Complex Systems and Their Applications (EDIESCA 2021).

Karimi, K., Zhand, S., Simons, G., Abdeldayem, W. S., Charalambous, N., & Giraud, I. (2025). Framing Evidence-Based Design and Planning: An Analytical, Multi-Scalar and Iterative Framework for Urban Design and Planning. *Urban Science*, *9*(11), 457.

Kemajou, A., Konou, A. A., Jaligot, R., & Chenal, J. (2021). Analyzing four decades of literature on urban planning studies in Africa (1980–2020). *African Geographical Review*, *40*(4), 425-443.

Kogan, F. (2023). The IPCC reports on global warming and land changes. In *Remote Sensing Land Surface Changes: The 1981-2020 Intensive Global Warming* (pp. 67-79). Springer International Publishing.

Li, C., Ma, Z., Wang, L., Yu, W., Tan, D., Gao, B., & Zhao, Y. (2021). Improving the accuracy of land cover mapping by distributing training samples. *Remote Sensing*, *13*(22), 4594.

Lillesand, T., Kiefer, R. W., & Chipman, J. (2015). *Remote sensing and image interpretation*. John Wiley & Sons.

Masoudi, M., Centeri, C., Jakab, G., Nel, L., & Mojtahedi, M. (2021). GIS-based multi-criteria and multi-objective evaluation for sustainable land-use planning (case study: Qaleh Ganj County, Iran). *International Journal of Environmental Research*, *15*(3), 457-474.

Mutale, M, and Ajayi, O. G. (2026). Gender responsive spatial analysis of climate impacts on land access in Windhoek. African Journal on Land Policy and Geospatial Sciences, 9(2), 308–339. https://doi.org/10.48346/IMIST.PRSM/ajlp-gs.v9i2.63096

National Population Commission (2006). Population Records, Niger State. Abuja: National Population Commission.
Nnanguma, K. A. (2025). Climate change and agriculture in Nigeria: Implications for Food Security and Rural Livelihoods. *International Journal of Intercultural Values and Indigenous Ecoethics.*
Nunes, C. A., Berenguer, E., França, F., Ferreira, J., Lees, A. C., Louzada, J., & Barlow, J. (2022). Linking land-use and land-cover transitions to their ecological impact in the Amazon. *Proceedings of the National Academy of Sciences*, *119*(27), e2202310119.
Pang, R., Hu, N., Zhou, J., Sun, D., & Ye, H. (2022). Study on eco-environmental effects of land-use transitions and their influencing factors in the Central and Southern Liaoning Urban Agglomeration. *Land*, *11*(6), 937.
Rezvani, S. M., de Almeida, N. M., & Falcão, M. J. (2023). Climate adaptation measures for enhancing urban resilience. *Buildings*, *13*(9), 2163.
Singh, K. T., Singh, N. M., & Devi, T. T. (2022). A remote sensing, GIS based study on LULC change detection by different methods of classifiers on Landsat data. In *Innovative trends in hydrological and environmental systems*. Springer Nature Singapore.
Sumari, N. S., Cobbinah, P. B., Tetteh, N., & Erdiaw-Kwasie, M. O. (2025). Unsettled urbanization: Spatiality of urban growth in Dodoma, Tanzania. *Geo-spatial Information Science*, 1-20.
Sumari, N. S. (2025). The Evolution of Urbanization in Dodoma: A 21-Year Spatial Assessment. *The International Archives of the Photogrammetry, Remote Sensing and Spatial Information Sciences*, *48*, 1397-1406.
Tefera, M. L., Carletti, A., Altea, L., Rizzu, M., Migheli, Q., & Seddaiu, G. (2024). Land degradation and the upper hand of sustainable agricultural intensification in sub-Saharan Africa–A systematic review. *Journal of Agriculture and Rural Development in the Tropics and Subtropics (JARTS)*, *125*(1), 63-83.
Wellmann, T., Lausch, A., Andersson, E., Knapp, S., Cortinovis, C., Jache, J., & Haase, D. (2020). Remote sensing in urban planning: Contributions towards ecologically sound policies? *Landscape and Urban Planning*, *204*, 103921.
Yasrebi, B., Abbasi, H., Behnamfar, K., & Dinarvand, M. (2025). Land use/Land Cover Dynamic Modeling Using RS and GIS with Emphasis on Maximum Likelihood Rule and Transition Matrix. *Ecopersia*, *10*(3), 191-202.
Yang, J., Zhang, Y., & Liu, Z. (2025). Urban expansion and its environmental impact in Xi'an, China. *Environmental Modelling & Software***,** 134, 104567.
Zhang, Y., Kwan, M. P., & Yang, J. (2023). A user-friendly assessment of six commonly used urban growth models. *Computers, Environment and Urban Systems*, *104*, 102004.

CONTACTS

Ekundayo Abayomi ADESINA
Department of Geomatics,
Faculty of Environmental Sciences,
University of Benin, Nigeria.
Tel. +234 803 809 5866
Email: ekundayo.adesina@uniben.edu

Oluibukun AJAYI
Department of Land and Spatial Sciences, Namibia University of Science and Technology
Department of Geography, Geoinformatics and Meteorology, University of Pretoria, South Africa
Email: oajayi@nust.na

Joseph ODUMOSU
Department of Land and Spatial Sciences,
Namibia University of Science and Technology
Email: jodumosu@nust.na